

J. L. Daniel ² and Shuichiro Takahashi ³Abstract

Experimental evidence has been obtained to demonstrate room temperature microplasticity of UO_2 . Electron microscopy of micro-hardness indenter marks shows increased dislocation etch pit densities, oriented slip bands, and definite plastic flow of the UO_2 . Single crystal fracture surfaces show similar evidence, but the effect appears to be overridden by other phenomena in irradiated polycrystalline UO_2 .

Introduction

UO_2 is usually considered to be a brittle material, and does behave so in normal applications. But "brittle" is a relative term, and depends partly on the frame of reference for measurement. It has been shown (1)(2)(3)(4) that UO_2 possesses microplasticity even at room temperature. Data on both single crystal and sintered UO_2 showed that the effect of compression stressing may be interpreted as due to plasticity resulting from multiplication and movement of dislocations under stress.

In the course of several research programs we have obtained further visual evidence of microplasticity in UO_2 at room temperature. It is of interest here to examine this evidence of microplasticity, consider how it may manifest itself generally in UO_2 , and note the way it may be strongly affected by low amounts of irradiation.

Experiments and Discussion

Most of this work has been on single crystals, prepared by arc fusion of high purity UO_2 in inert atmosphere. Such material is nearly stoichiometric ($2.00 \pm .005$), of high purity (~ 200 ppm impurity, comprising mainly C, N, Fe and Al), and low porosity (99 + % of theoretical density)(Table I). It should be recognized that on a microscale each grain of a polycrystalline solid will behave to some extent like the single crystal.

-
- 1 Work performed in part under U.S. Atomic Energy Commission Contract AT(45-1)1830 and the program of the Japan-U.S. co-operative study of nuclear fuels.
 - 2 Battelle Memorial Institute, Pacific Northwest Laboratories Richland, Washington, USA
 - 3 Mitsubishi Atomic Power Ind., Inc., Engineering and Research Laboratory, Ohmiya City, Saitama, Japan

A typical single crystal cleavage surface obtained by impact fracture is shown in Fig.1. Natural cleavage of UO_2 occurs on the (111) plane, and is influenced by minor impurities and by the residual stresses resulting from the rapid cooling used in fabrication. Solidification after fusion may occur stepwise, perhaps resulting in the layered structure shown along one edge of this specimen; this layering effect is not normally encountered, however. Looking at the fracture surface a little more closely, using reflection electron microscopy of a freshly fractured specimen (Fig.2 and 3), it is readily evident that a variety of fracture modes may occur on a single specimen, the predominant type displaying the typical steps and river patterns of Fig.3. There is nothing immediately evident here to suggest the presence of plastic flow, but fracturing by impact does not lend itself to observation of micro effects. However, a microhardness diamond point indenter, as used by Honda, et al.(3) provides an easily controlled method of introducing local concentrated stresses and defect structure. Applied stress will vary continuously, from a maximum at the instant of point contact, to the minimum at the final indenter position; both plastic and elastic deformations may contribute to the final indent size. The approximate minimum pressure may be calculated from the applied load and the indented surface area; for these tests the calculated pressure was of the order of 10^4 kg/cm² (Table II). Indenting a single crystal fracture surface with an equiaxial (Vickers) diamond point using a 300 g load at room temperature and subsequently etching, a combination of microcracking and microplasticity is revealed by the dislocation etch pits (Fig.4). The dislocations extend 25 to 100 microns from the indent edges, about twice as far as the longest microcrack. In some regions the triangular array typical of the (111) planes of UO_2 is apparent.

The dislocation density is pressure and temperature dependent (Fig.5), probably accounting in part for the observations that microhardness values are very sensitive to the indenter load(5). Indenting at 200°C produces the regular array of well defined etch pits shown in the top figure; alignment and distribution again are typical of (111) UO_2 planes. Indentation at 500°C (center micrograph) increases the dislocation density by about 10 times; the step passing through the area appears to have no effect on dislocation density. However, nearly all these dislocations can be annealed out at 1500°C in 1 hour or less (lower micrograph) (Table II).

This technique may be taken a step further by applying a Knoop diamond-shaped indenter to a polished single crystal surface, controlling the indenter orientation(5). Using a 1000 gram load, and with the long axis of the indenter parallel to the direction of intersection of (111) and (100) planes of the crystal, slip bands result parallel to the indenter, and cracking is minimal (Fig.6, upper micrograph). On the other hand, rotation of the specimen by 30° (lower figure 6) leads to much more extensive microcracking, and again slip lines corresponding to the main crystallographic directions of the UO_2 crystal. Etching (Fig.7) shows the extent of dislocation formation more clearly. Nearly all the dislocations occurred along the slip lines evident before etching, for a distance of about 50 microns, 4 or 5 times the width of the indentation.

The evidence shown so far relies entirely on dislocation multiplication and slip line formation, and the assumption that these are manifestations of plasticity. Direct observations of plastic flow under the stressing of the diamond indenter can be achieved by use of reflection electron microscopy (Fig.8). In this case a 100 g load was applied, resulting in a smaller indentation with no cracking. Using a 17° angle of specimen tilt in the electron microscope, the raised lips of the indentation are readily seen. The indentation is about 35 microns long and 10 microns wide; the UO_2 edges have extruded 2 or 3 microns above the original specimen surface. In addition, slip lines can be seen extending from one end of the indentation. It is obvious that plastic flow has occurred, under conditions very similar to those producing dislocation etch pits in the previous examples.

Let us now consider the significance of these observations in the interpretation of the general behavior of UO_2 specimens. Examination of the etched fracture surface of a UO_2 single crystal shows several features similar to those produced by the diamond indenter (Fig.9). In particular, impurity inclusions are surrounded by dislocation etch pits, suggesting that some plastic flow occurred at that point. Similarly, etch pits are found along fracture steps, indicating that microplasticity may have permitted a limited plastic deformation in the vicinity of the fracture step preceding final fracture. Electron micrographs of replicas show that the fine detail of apparent slip lines includes etch pit structure similar to that introduced by the diamond indenter (Compare Fig.5 and 9).

Sintered polycrystalline UO_2 presents a more complicated problem of interpretation; the fracture behavior has not been studied in sufficient detail for complete understanding. However, on a micro scale the individual grains may be considered as separate crystals, undoubtedly influenced to some extent by the adjacent grain boundaries. On a fracture surface (Fig.10) the typical river pattern structure (6)(7) is observed in the nonetched surface. The observations that pores and small amounts of impurities play a significant role in the occurrence of fracture, and that fracture ordinarily considered "brittle" may involve localized plastic flow on a micro scale immediately preceding fracture, suggest that in the transgranular fracture normally occurring in sintered UO_2 as shown here the sites of impurity inclusions may have been centers of plastic flow initially.

Upon irradiation (right micrograph), the fracture changes to primarily intergranular. Apparently the fission products which are formed, and the porosity initially present, tend to agglomerate in grain boundaries during irradiation; on subsequent stressing these areas serve as sites of fracture initiation. Probably microplastic deformation also occurs with intergranular fracture, but the other effects causing grain boundary weakening may predominate.

Although most observers have found that the fracture character generally changes from transgranular to intergranular upon irradiation, other types of changes may occur as well. For example (Fig.11), both of these specimens received about 1.5×10^{19} fissions/cc. No river patterns typical of transgranular fracture occur in either, but while one appears to be a rather featureless transgranular fracture, the other is distinctly intergranular. The reason for the difference in behavior is not understood, but may stem from differences in initial material or irradiation conditions, including irradiation time, temperature, and flux rate.

Conclusions

It has been demonstrated that "brittle" UO_2 actually displays microplasticity behavior, with dislocation movement on the order of 100 microns at room temperature; this plasticity appears to influence the fracture characteristics of the material. It is reasonable to expect a similar microplasticity to occur in other brittle materials as well. More study will be required to evaluate the role of this plasticity in fracture behavior under complicated conditions such as in polycrystalline materials or upon irradiation.

Acknowledgements

The authors are indebted to Dr. J. L. Bates for use of some of his unpublished micrographs particularly pertinent to this work.

The authors express also their thanks to Messrs Y. Honda, S. Nagata and B. Ishii for help in this experimental work.

References

1. Yokosuka, M., Takahashi, S., Honda, Y. and Seki, Y., Fuel Element Fabrication, Vol.2, p.55, Academic Press (1961)
2. Honda, Y., Takahashi, S., J. Japan Inst. Metals (in Japanese), Vol.27, p.357 (1963), also Trans. Japan Inst. Metals (in English), Vol.5, p.177 (1964)
3. Honda, Y., Nagata, S., Takahashi, S., J. Japan Inst. Metals (in Japanese), also Trans. Japan Inst. Metals (in English), (to be published)
4. Igata, N., Hasiguti, R. R., and Domoto, K., International Conference on Fracture, Sendai (1965)
5. Bates, J. L., USAEC Report HW-77799, (June 1963)
6. Bates, J. L. and Daniel, J. L., American Ceramic Society Annual Meeting, 1965, (to be published)
7. Newkirk, H. W., Daniel, J. L. and Mastel, B., J. Nuc. Materials, Vol.2, pp.269-273 (1960)

Table ITypical Analysis of Arc Fused UO_2 Crystal

Al	-	20 ppm
Fe	-	50 ppm
C	-	40 ppm
N	-	40 ppm

Sum of all other metallic impurities: 100 ppm

O/U	-	2.004±.005
Density	-	10.96 g/cc

Table IIDislocation Density and Plasticity in Indented UO_2 (3)

(Specimen: Arc fused single crystal UO_2 , cleavage surface)

<u>Indent Test Temperature</u>	<u>Calculated Minimum Mean Pressure</u> ^{1/}	<u>Post-Indent Annealing</u>	<u>Dislocation Density(Avg.)</u>	<u>Plasticity</u> ^{2/}
Initial specimen	-	-	$8.5 \times 10^6 \text{ cm}^{-2}$	-
20°C	$6.5 \times 10^4 \text{ kg/cm}^2$	none	1.9×10^7	$2.5 \times 10^{-2} \text{ mm}$
200°	4.1×10^4	none	5.4×10^7	3.6×10^{-2}
500°	2.4×10^4	none	2.1×10^8	6.7×10^{-2}
500°	2.4×10^4	1300°C, 1 hour	6.4×10^7	-
500°	2.4×10^4	1500°C, 1 hour	1.5×10^7	-

$$\frac{1/}{\text{Indenter load}} = \frac{300 \text{ g}}{\text{Indent Mark Area} \times \text{Indent Mark Area}}$$

^{2/} Average distance from the edge line of indentation to the outer slip line.

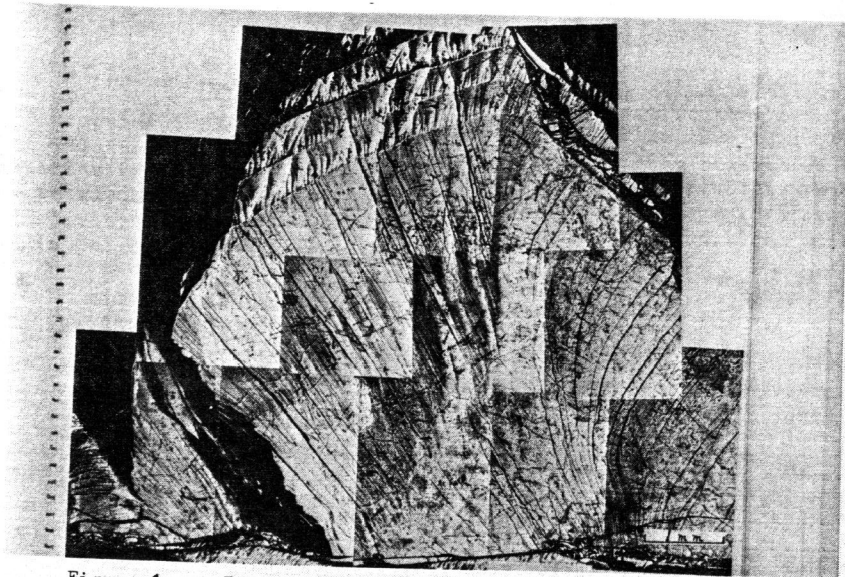


Figure 1 Typical Cleavage Surface of Arc-Fused Uranium Dioxide Single Crystal. Layered structure along one edge occurs occasionally, and may result from step-wise cooling of the fused melt.

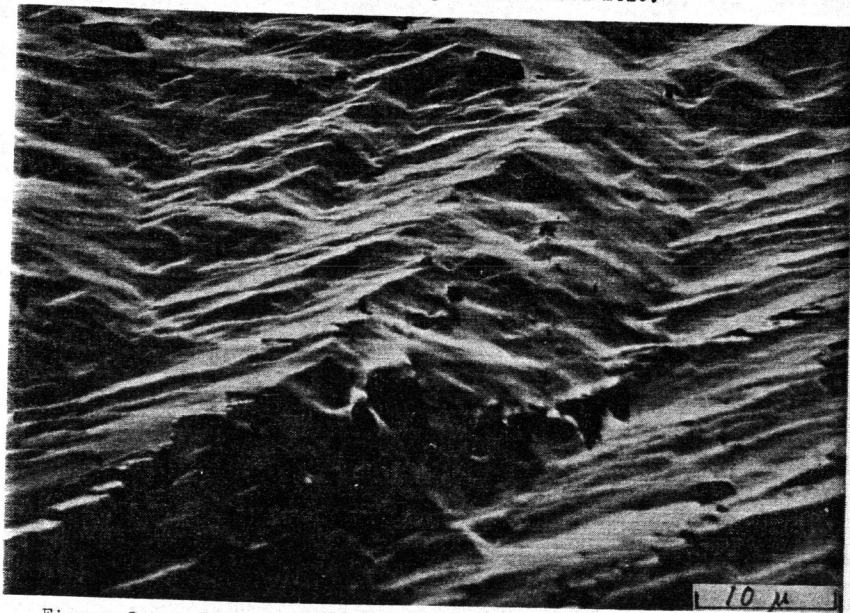


Figure 2 Cleavage Surface of UO₂ Single Crystal (Reflection Electron Microscopy). One of two most common surface structures encountered.

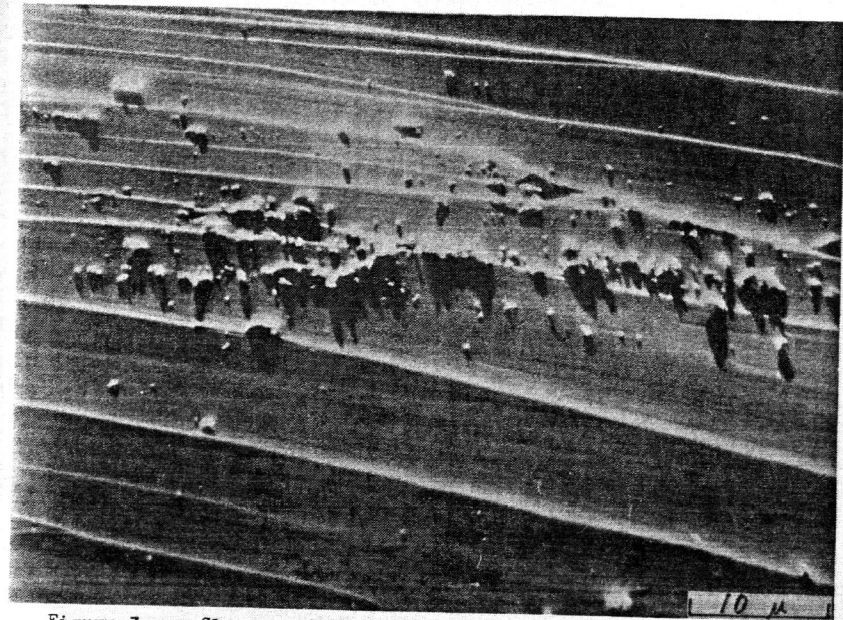


Figure 3 Cleavage Surface of UO₂ Single Crystal (Reflection Electron Microscopy). Most common cleavage surface structure.

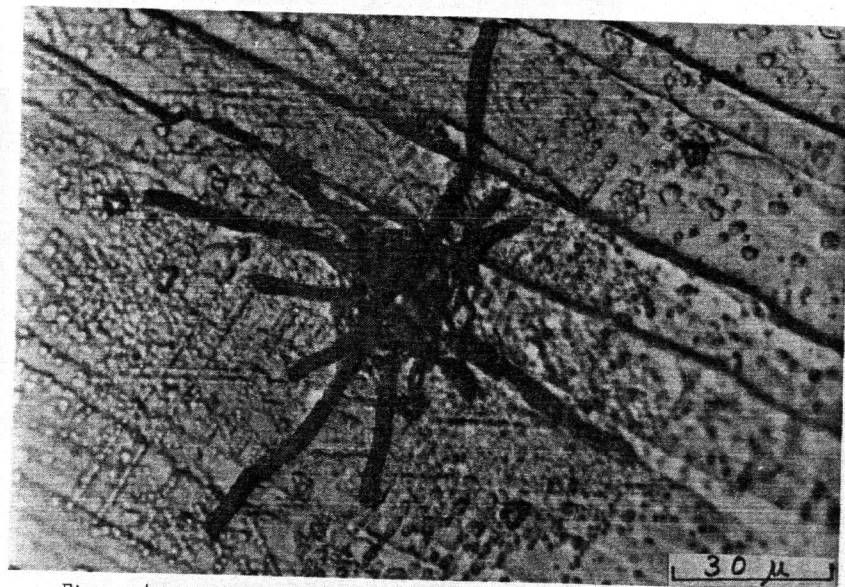


Figure 4 Micrograph of UO₂ Fracture Surface (111 plane) after Diamond Indentation at 200C, and Subsequent Etching (300 gram load)

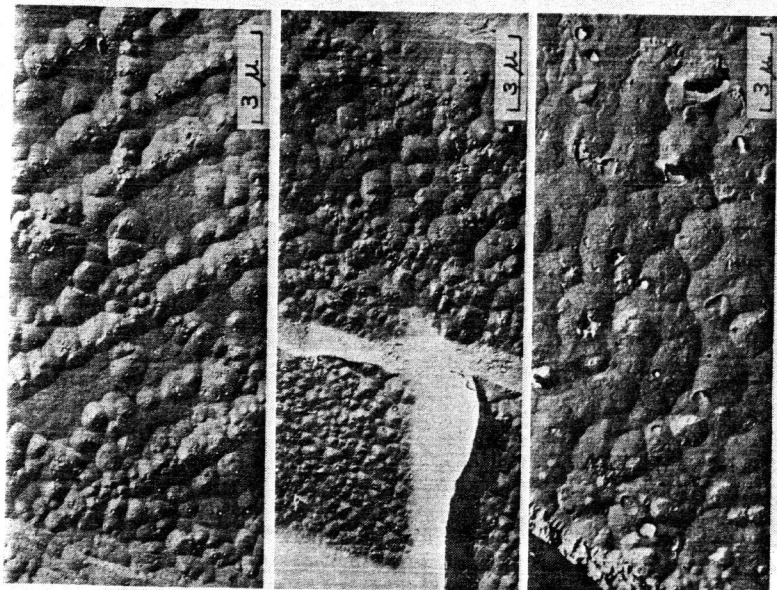


Figure 5 Temperature Effect on Dislocation Density Produced by Diamond Indentation (300 G Load)

Top: Indented at 200°C; etched
 Middle: Indented at 500°C; etched
 Lower: Indented at 500°C and annealed at 1500°C for 1 hour; etched

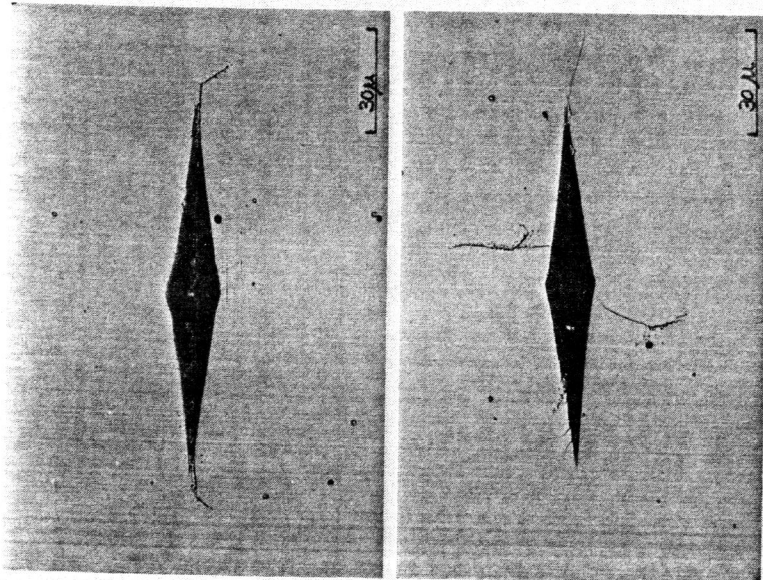


Figure 6 Indentation by Knoop Indenter (100 G Load) on Polished (111) Plane of UO₂ Single Crystal

Upper: Indenter axis parallel to direction of intersection of (111) and (100) crystal planes
 Lower: Same Crystal rotated 30° from original position

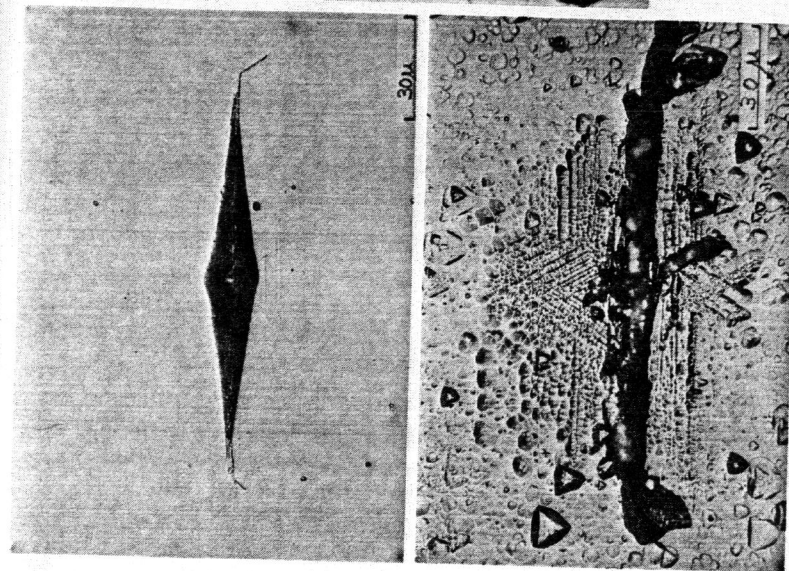


Figure 7 Knoop Indentation on (111) Plane of UO₂ Single Crystal

Upper: As indented on polished surface
 Lower: After etching

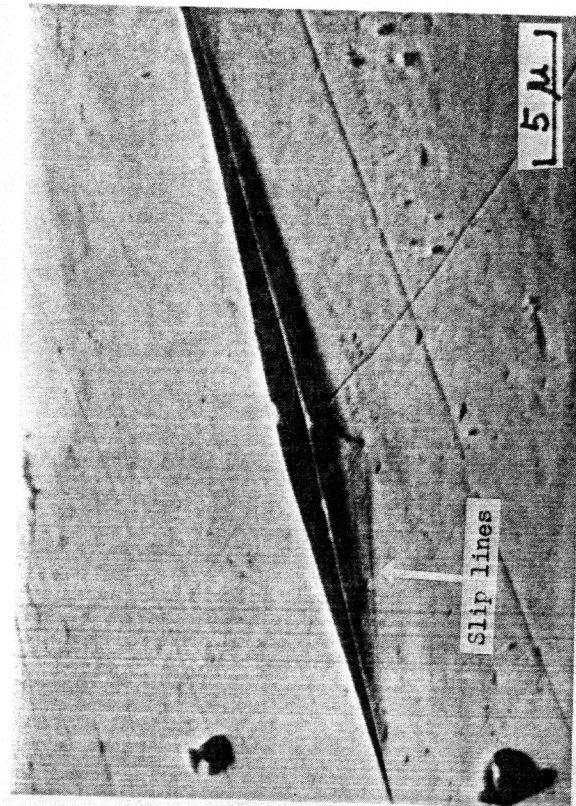


Figure 8

Indentation on Polished (111) UO₂ Plane (100 G Load), showing material extruded by pressure of the indenter (Reflection electron micrograph; specimen angle 17°). Note the slip lines extending from the left end of the indentation.

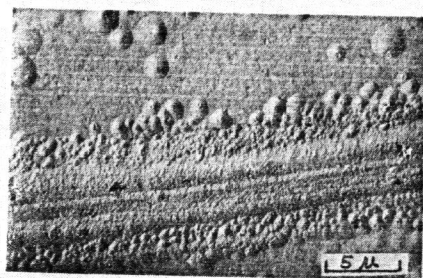
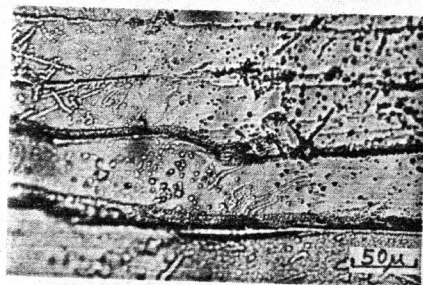
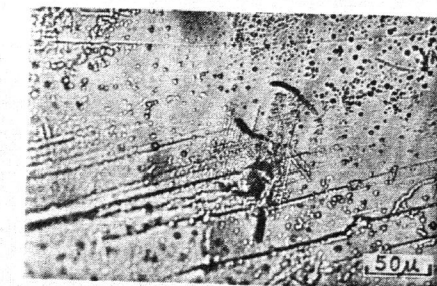


Figure 9 Dislocation Etch Pits on UO₂ Cleavage Surface

Upper: Impurity inclusion
 Middle: Slip lines
 Lower: Microslip lines

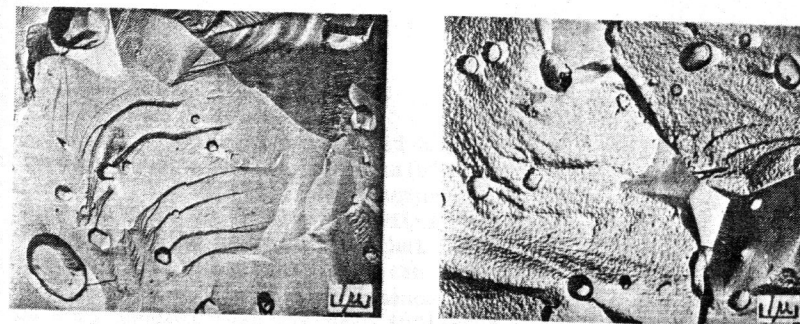


Figure 10 Polycrystalline UO₂ After Fracture

Left: As fabricated by pressing, and sintering at 1700°C in hydrogen
 Right: After low-flux irradiation to 1.4×10^{19} f/cc; Maximum irradiation temperature < 100°C

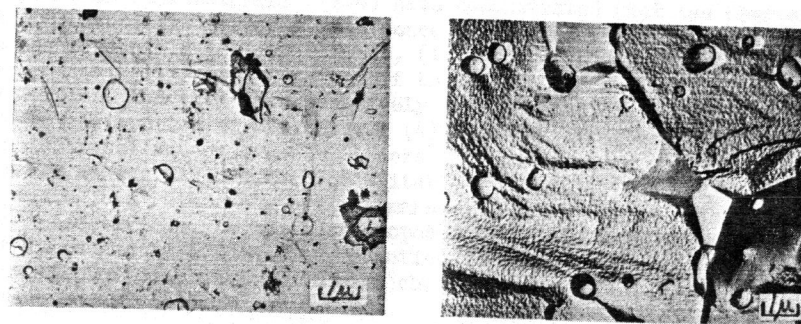


Figure 11 Irradiated Polycrystalline UO₂

Left: 1.7×10^{19} f/cc; irradiated at temperatures 400° - 900°C
 Right: 1.4×10^{19} f/cc; irradiated at temperature < 100°C
 (Specimens prepared independently from different starting materials.)